

NASA Technical Paper 1442

LOAN COPY: RETURN TO  
AFWL TECHNICAL LIBRARY  
KIRTLAND AFB, N.M.



# Wear of Aluminum and Hypoeutectic Aluminum-Silicon Alloys in Boundary-Lubricated Pin-on-Disk Sliding

John Ferrante and William A. Brainard

APRIL 1979

**NASA**





NASA Technical Paper 1442

# Wear of Aluminum and Hypoeutectic Aluminum-Silicon Alloys in Boundary- Lubricated Pin-on-Disk Sliding

John Ferrante and William A. Brainard  
*Lewis Research Center*  
*Cleveland, Ohio*



National Aeronautics  
and Space Administration

**Scientific and Technical  
Information Office**

1979

## SUMMARY

The friction and wear of pure aluminum and a number of hypoeutectic aluminum-silicon alloys (with 3- to 12-wt% Si) were studied in a pin-on-disk apparatus. The contacts were lubricated with mineral oil and sliding was in the boundary-lubrication regime at 2.6 centimeters per second. Surfaces were analyzed with photomicrographs, scanning electron microscopy, X-ray dispersive analyses, and diamond pyramid hardness measurements. There were two wear regimes for the alloys - high and low - whereas pure aluminum exhibited high wear throughout the test period. Wear rate decreased and the transition stress from high to low wear increased with increasing hardness. There was no correlation between friction coefficient and hardness. A least-squares curve fit indicated a wear-rate dependence greater than the inverse first power of hardness. The lower wear rates of the alloys may be due to a composite of silicon platelets in aluminum resulting in increased hardness and thus impairing the shear of the aluminum.

## INTRODUCTION

Aluminum-silicon alloys are widely used in internal-combustion engines as cylinder blocks, cylinder heads, and pistons (ref. 1). More recently, these alloys have been used as rocker-arm pivots in internal-combustion engines. In spite of the importance of these alloys, little effort has been expended in studying their wear (ref. 2), although considerable effort has been expended in studying aluminum (ref. 3). In addition, there seem to be no studies of lubricated Al-Si alloys, the condition normally encountered in practical applications. Sarkar (ref. 1) studied two alloys, Al - 11-wt% Si and Al - 22-wt% Si, under dry conditions with the principal objective of determining the dependence of alloy wear rate on load. He makes no comment on the effect of Si content, other than that the hypereutectic alloy has a higher wear rate than the hypoeutectic. Sarkar, in citing other work in the literature, points out contradictory results: Some publications state that the distribution of Si particles is important; others conclude that the distribution is unimportant and only the total Si content is important. Shivanatha, et al. (ref. 2) also report studies of hypoeutectic Al-Si alloys under dry sliding conditions. They observed two wear regimes, oxidative and metallic, and found no correlation between mechanical properties or Si content and the particle-size distribution in the metallic regime. Because of the lack of studies on lubricated Al-Si alloys

and the contradictory results concerning Si content in dry sliding, further study of these alloys under lubricated conditions is warranted.

The present study was conducted to examine the wear of a number of hypoeutectic Al-Si alloys (with 3- to 12-wt% Si) and to compare these results with that for pure Al. Wear was studied in a pin-on-disk experiment with the Al or alloy pin sliding on an AISI 52100 steel disk. The specimens were lubricated with mineral oil in air with controlled humidity (15-percent relative humidity) at room temperature. A sliding speed of 2.6 centimeters per second was selected so that the experiments would be conducted in the boundary-lubrication regime. Wear-scar diameters were measured at various sliding distances for each material. Wear rates were calculated by using a least-squares curve fit (ref. 4). The friction coefficient was continuously recorded during sliding. The surfaces were examined with scanning electron microscopy (SEM), X-ray dispersive analysis (XDA), photomicrographs, and diamond pyramid hardness measurements.

## EXPERIMENTAL PROCEDURE

The wear studies were performed in the pin-on-disk apparatus shown in figure 1. The angular speed of the disk and the load of the pin against the disk could be varied. The frictional force was continuously measured by a beryllium-copper strain gage mounted tangential to the disk. The friction-and-wear apparatus was placed in a Plexiglass box in order to achieve some environmental control. A desiccant was placed in the box to maintain 15-percent relative humidity. A 500-gram load was used to ensure that boundary lubrication could be obtained under these conditions. The rotational speed of the disk was selected by reducing its speed until the friction coefficient rose. This procedure eliminated elasto-hydrodynamic effects and ensured boundary lubrication. At the point of contact the sliding speed was 2.6 centimeters per second.

The experiment was performed by sliding a pin on an AISI 52100 disk and continuously measuring the friction force. At preselected times the tests were stopped and pin wear was determined by measuring the wear-scar diameter. After the wear test the microhardness was measured within the wear scar by using a diamond pyramid hardness tester with a 150-gram load. Typically, the scatter in the hardness measurement was  $\pm 10$  percent. The value reported is an average of three measurements.

Before and after the wear tests, the alloys were examined with a scanning electron microscope and by X-ray dispersive analysis. The Al-8Si alloy, which is used in commercial applications, was also examined during the wear test by removing it from the pin-on-disk apparatus, cleaning it, and placing it in the vacuum chamber of the electron microscope.

## MATERIALS

The Al-Si alloy pins were fabricated by casting an Al - 12-wt%-Si brazing wire. The composition of the brazing wire was nominally (in wt%) 86.45Al-12Si-0.8Fe-0.3Cu-0.2Zn-0.15Mn-0.1Mg. This alloy was fused and diluted with 99.999-percent-pure Al to form alloys of the following nominal compositions (in wt%): Al-12Si, Al-10Si, Al-8Si, Al-6Si, and Al-3Si. The alloys were fused in an iron ladle, poured into a Vycor mold placed in sand, and then air cooled. Photomicrographs of metallographically prepared specimens from these alloys are shown in figures 2(a) to (d) and (f). The background is uniform and has a two-phase eutectic structure. In addition, pure Al, an alloy of Al - 9.9-wt% Si - 1-wt% Sr, and a commercial alloy of nominally Al - 8-wt% Si - 1-wt% Cu were examined. The strontium-modified alloy (fig. 2(e)) showed a considerably different, strong dendritic microstructure. A phase diagram for the Al-Si system is shown in figure 3, with composition lines for each alloy studied.

The alloys were machined into cylinders 0.95 centimeter in diameter; a 0.95-centimeter-diameter hemisphere was machined on the end of each cylinder, forming a pin. The pins were then polished with 1-micrometer alumina and electropolished in orthophosphoric acid. A SEM photograph of the Al-8Si alloy (fig. 4(a)) shows that part of the surface was attacked by electropolishing but that the raised portions were not attacked. An XDA analysis of the same area (fig. 4(b)) shows that the raised portions had a high silicon concentration. This result was typical of the results for the other alloys examined.

Pins of these alloys were run against a hardened AISI 52100 disk with a diameter of 6.25 centimeters and a nominal composition (in wt%) of Fe-0.94C-0.34Mn-0.27Si-0.95Cr. The disk was given its final finish on a vibratory polisher with 0.3-micrometer alumina. The disk was degreased in a fluorocarbon solvent after polishing. The polishing and cleaning procedures were repeated after each wear test. The lubricant used in the study was white mineral oil with a viscosity of  $0.0662 \pm 0.00026$  N·sec/m<sup>2</sup> at 37.8° C and an impurity level less than 100 parts per million. The lubricant was puddled on the surface rather than placed in a cup. The rotational speed of the disk was sufficiently low to maintain the liquid at a uniform thickness on the disk.

## ANALYSIS

The wear rates of the alloy were analyzed by using Archard's equations (ref. 5)

$$V = \frac{KWL}{H^n} \quad (1)$$

$$\frac{dV}{dL} = \frac{kW}{H^n} \quad (2)$$

where  $V$  is the volume of material worn away,  $K$  is a constant,  $W$  is the load,  $L$  is the sliding distance,  $H$  is the hardness, and  $n = 1$  is the exponent typically used in this relationship. This point is discussed in more detail in the section DISCUSSION. In general, time was used in the analysis rather than sliding distance. Since the disk was rotated at a constant angular speed  $\omega$ , the two quantities are equivalent. That is,  $L = \omega r t$ , where  $r$  is the radius of the wear track and  $t$  is the time. The results were analyzed by determining the wear volume as a function of time. These wear volumes were curve fit, by using the method of least squares, to equation (1). From these curve fits the wear rate was determined. The wear rate was then curve fit to equation (2) with hardness as the independent variable.

## RESULTS

A typical plot of wear volume as a function of time (sliding distance) for an aluminum alloy is shown in figure 5. All the alloy pins showed the same wear behavior; namely, there was a high initial wear rate and then a transition to a low-wear-rate regime. Both regimes appeared to have a linear dependence on sliding distance, in agreement with equation (1). The solid lines in the figure were obtained by performing a least-squares curve fit to each region. (A summary of wear rates and hardness for each material is presented in table I.) The slopes of these lines define the wear rate. The intersection of these lines defines the transition point from a high-wear-rate regime to a low-wear-rate regime. For pure Al, no transition to a low-wear-rate regime was observed in the 24-hour test period (fig. 6).

The wear rate in the high-wear-rate regime is shown as a function of Si content and hardness, respectively, in figures 7(a) and (b). There is considerable scatter in the correlation between wear rate and Si content, but the correlation between wear rate and hardness is much better. In general, wear rate decreased with increasing hardness. Included in figure 7(b) is a least-squares curve fit of wear rate as a function of hardness. In performing the curve fit the log of the wear rate was used to properly weight the data, which ranged over two orders of magnitude. The corresponding plots for the low-wear-rate regime are shown in figure 8. The behavior in this regime was like that in the high-wear-rate regime; that is, wear rate decreased with hardness and a better correlation was obtained with hardness than with Si content.

Friction coefficient as a function of wear rate, Si content, and hardness, respectively, is shown in figures 9(a) to (c). The bars represent the deviation of the friction coefficient about its mean value as shown in figure 9(d). There was no difference in

friction coefficient between the low- and high-wear-rate regimes. As might be expected, there was little or no correlation between the friction coefficient and any of these quantities.

The apparent transition stress (load divided by wear-scar area) as a function of hardness at the transition between the high- and low-wear-rate regimes is shown in figure 10. The transition stress was obtained by determining the wear volume at which the linear curve fits to the high- and low-wear-rate regimes intersected. From this an apparent contact area was obtained that was divided into the load. An SEM photograph of the wear scar for the Al-8Si alloy (fig. 11(a)) is typical of results for the other alloys and is representative of the commercial alloys. An XDA image of the Si contact in the same region is shown in figure 11(b). There is a similarity between the structures shown in figure 2 and the compositional structure below the wear scar shown in figure 11(b). (XDA samples a region extending a micrometer below the surface.)

SEM photographs of the Al-8Si alloy are shown in figures 12(a) to (c) for the same region of the wear scar but for increasing sliding distances (200, 2000, and 3000 revolutions). The same wear-scar region is shown after electropolishing, which selectively attacks the Al, in figure 12(d). An Si XDA image of the same area after 3000 revolutions is shown in figure 12(e). Because the raised portion of the pin shown in figure 12(e) was principally Si, the Al was probably smeared over and in between the Si platelets during sliding. Because the AISI 52100 disk had a raised portion after sliding, a transfer film was probably formed from the pin to the disk.

## DISCUSSION

The wear of Al-Si alloys in lubricated contacts has been studied and compared with the wear of pure Al to provide useful information about these little-studied but important alloys. The emphasis in the present study is on the effect of material properties on wear. Consequently, the lubricant was kept constant and hydrodynamic effects were minimized by selecting a low enough sliding speed.

The wear of Al-Si alloys in lubricated contacts, as compared with the wear of pure Al, has some interesting features. The alloys progressed from a high-wear-rate region to a low-wear-rate region. Pure Al continued to have a high wear rate throughout the tests (figs. 5 and 6). The wear rate of pure Al was one to two orders of magnitude higher than those of the alloys. This behavior is possibly related to the nature of the pin-on-disk experiment in that the initially high apparent contact stress diminishes, as the pin wears, to below the yield stress and thus shear in the pin occurs less readily (ref. 6). Figure 10 shows behavior consistent with this reasoning since the transition stress increased with the hardness; that is, the harder the material the smaller the

wear scar when transition occurred. However, because the magnitude of the transition stress is much smaller than the magnitude of the hardness, asperity contacts probably dominate. Chemical effects such as oxidative wear or lubricant interactions may influence wear behavior and can be examined by performing similar experiments in an inert atmosphere.

An argument supporting a mechanical explanation for the results is shown in figures 7 and 8. As stated earlier, the wear rate correlated better with hardness (mechanical property) than with composition (chemical property) in the sense that the scatter in the data was less. A least-squares curve fit of wear rate to hardness (fig. 8) was performed for two reasons: The first reason was to provide a quantitative relationship for estimating wear for a given Al-Si alloy as an aid in predicting wear and in selecting materials. The second reason was to examine the dependence of wear on hardness quantitatively with regard to Archard's wear equations. In these alloys the exponent  $n$  is greater than 1.0 in both the high and low wear regimes. Consequently, although the correlation between wear and sliding distance agrees well with Archard's equations and wear is inversely dependent on hardness, the exponent is not in agreement with those equations. This result is not necessarily surprising since Archard's equations were derived for dry sliding. Similar observations have been made by Rabinowicz (ref. 7) for abrasive wear. No explanation is offered here for this behavior.

That the friction coefficient is not a good indicator of wear (fig. 9) was expected. In addition, no correlation of friction coefficient with hardness or composition was found.

An SEM photograph of the wear scar for the Al-8Si alloy and an XDA image of the same region showing the locations of silicon are presented as figures 11(a) and (b). Interestingly, the XDA structure looks very similar to the photomicrographs shown in figure 2. This suggests that wear does not disrupt the underlying structure. To further explore this observation we examined the same region of the wear scar as a function of sliding distance for the same alloy (fig. 12). The pin was then electropolished and XDA analyzed. The SEM photographs (figs. 12(a) to (c)) show the wear scar increasing in size from 200 to 2000 revolutions with, however, only a small change from 2000 to 3000 revolutions. An XDA image (fig. 12(e)) of the electropolished alloy (fig. 12(d)) shows that Al was smeared during sliding in between the Si platelets, which can be oriented vertically as shown in figure 4.

The dependence of alloy wear resistance on hardness can be explained by imagining that the alloy is a composite structure. The harder Si platelets act as a barrier to shear in the softer Al matrix and result in low wear. Increased hardness is possibly an indication of increased availability of the Si composite structure needed for increased shear resistance and thus low wear.

## CONCLUDING REMARKS

Comparing the wear of aluminum-silicon alloys with that of aluminum reveals some interesting features. The alloys go from a high- to a low-wear-rate regime with sliding distance. Aluminum, however, maintains a high wear rate over the entire sliding distance examined. Wear rate and the transition stress in going from high to low wear correlate with hardness. There seems to be little correlation between wear rate, silicon content, or hardness and the friction coefficient.

Examining the wear scars and surfaces with SEM and XDA before and after sliding suggests some wear mechanisms. The low wear in the aluminum-silicon alloys may be related to their composite structure, that is, their eutectic composition, where vertical platelets of silicon impair the ability of the intervening aluminum to shear.

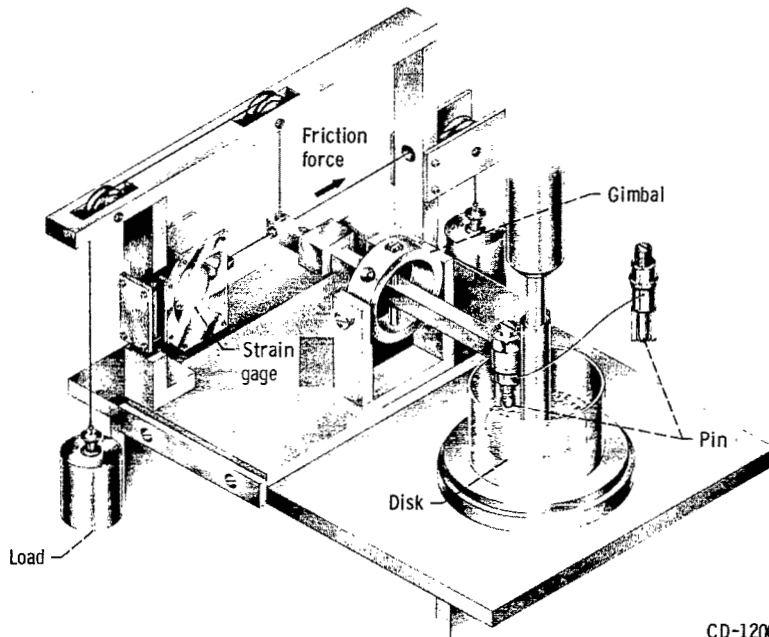
Lewis Research Center,  
National Aeronautics and Space Administration,  
Cleveland, Ohio, November 21, 1978,  
506-16.

## REFERENCES

1. Sarkar, A. D.: Wear of Aluminum-Silicon Alloys. *Wear*, vol. 31, 1975, pp. 331-343.
2. Shivanath, R.; Sengupta, P. K.; and Eyre, T. S.: Wear of Aluminum-Silicon Alloys. *Wear of Materials*. W. A. Glaeser, K. C. Ludema, and S. K. Rhee, eds., The American Society of Mechanical Engineers, 1977, pp. 120-126.
3. Montgomery, R. S.: Lubrication of Bearing Aluminum with Polyphenyl Ethers. *Wear*, vol. 14, 1969, pp. 213-217.
4. Scarborough, James B.: *Numerical Mathematical Analysis*. Third ed. Johns Hopkins Press, 1955, ch. XVI.
5. Archard, J. F.: Contact and Rubbing of Flat Surfaces. *J. Appl. Phys.*, vol. 24, no. 8, Aug. 1953, pp. 981-988.
6. Bowden, Frank P.; and Tabor, D.: *The Friction and Lubrication of Solids*. Part II. Oxford University Press (London), 1964, ch. IV.
7. Rabinowicz, Ernest: Abrasive Wear Resistance as a Materials Test. *Lubr. Eng.*, vol. 33, no. 7, July 1977, pp. 378-381.
8. Hansen, Max: *Constitution of Binary Alloys*. McGraw-Hill Book Co., Inc., 1958, p. 133.

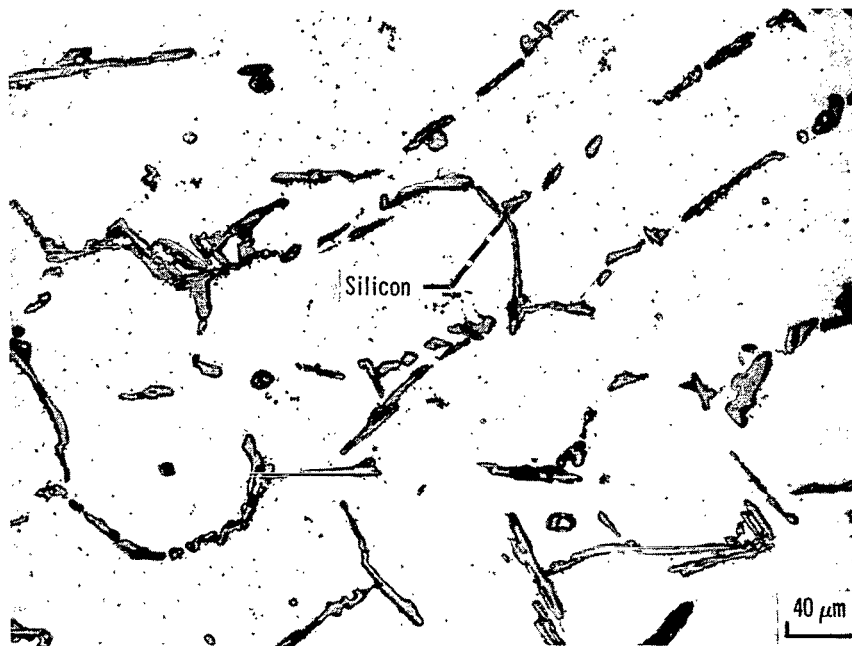
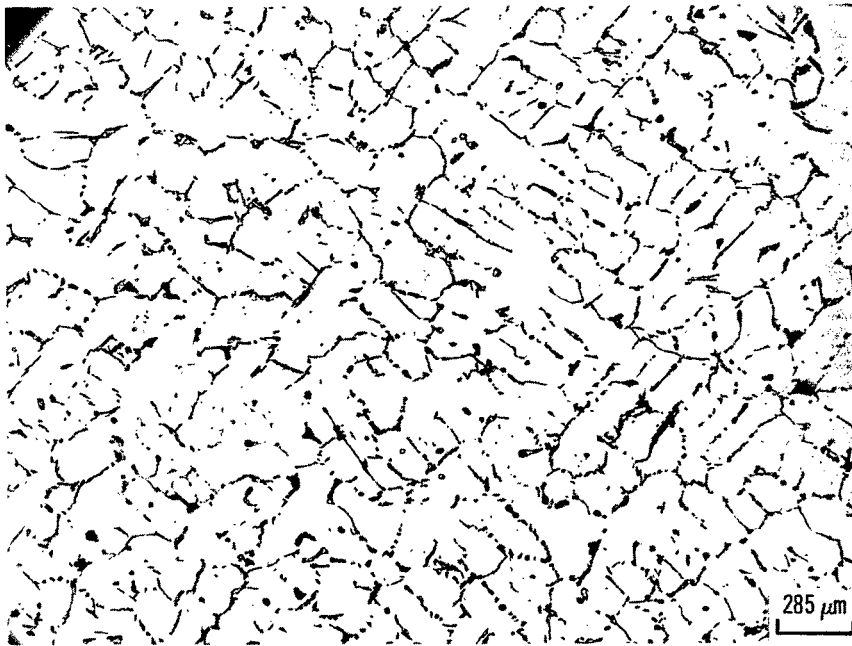
TABLE I. - HARDNESS AND WEAR RATES OF  
ALUMINUM-SILICON ALLOYS

Alloy, wt%	Diamond pyramid hardness, kg/mm <sup>2</sup>	Wear rate, cm <sup>3</sup> /hr	
		High	Low
Pure Al	20	$1.6 \times 10^{-5}$	-----
Pure Al	26	$1.2 \times 10^{-5}$	-----
Pure Al	25	$5.8 \times 10^{-6}$	-----
Al-3Si	32	$4.1 \times 10^{-6}$	$4.6 \times 10^{-7}$
Al-6Si	36	$6.0 \times 10^{-6}$	$2.5 \times 10^{-6}$
Al-6Si	36	$1.9 \times 10^{-6}$	$2.7 \times 10^{-7}$
Al-8Si	54	$2.3 \times 10^{-6}$	$4.6 \times 10^{-8}$
Al-8Si (not electropolished)	50	$1.4 \times 10^{-6}$	$5.9 \times 10^{-8}$
Al-8Si (commercial)	60	$3.1 \times 10^{-7}$	$5.9 \times 10^{-8}$
Al-10Si	44	$4.2 \times 10^{-6}$	$7.3 \times 10^{-7}$
Al-10Si (strontium modified)	49	$2.5 \times 10^{-6}$	$4.1 \times 10^{-8}$
Al-12Si	56	$2.3 \times 10^{-6}$	$4.6 \times 10^{-8}$



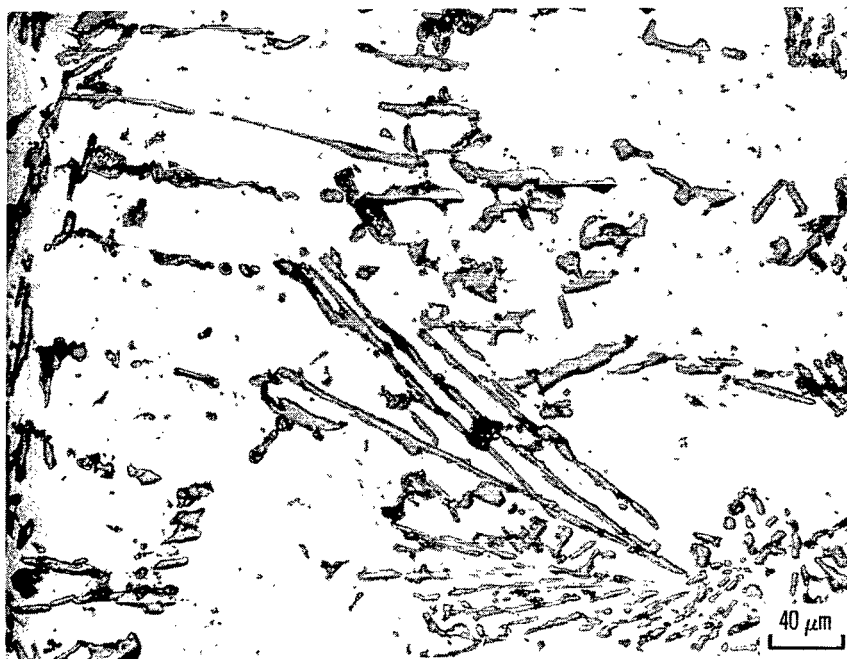
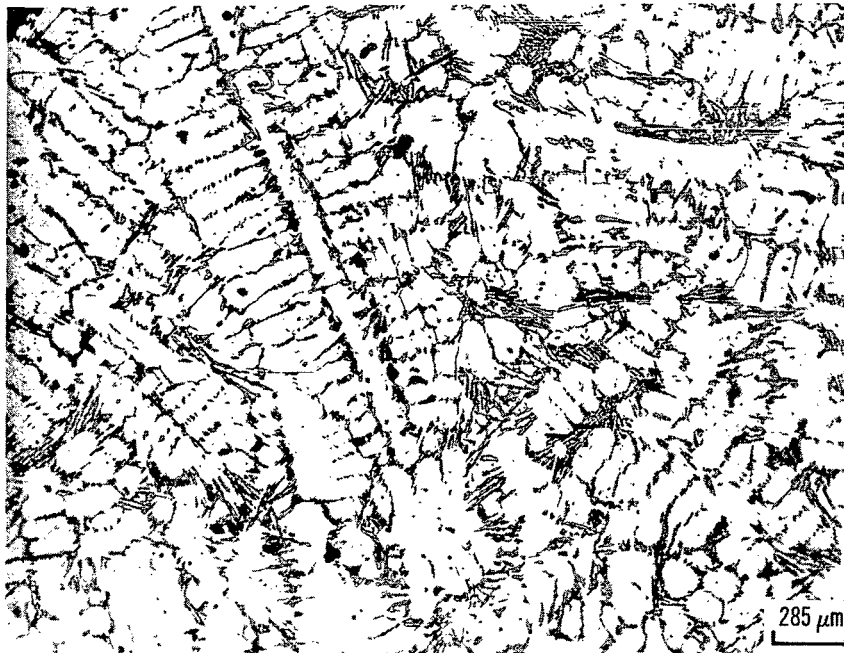
CD-12001-26

Figure 1. - Pin-on-disk friction and wear apparatus.



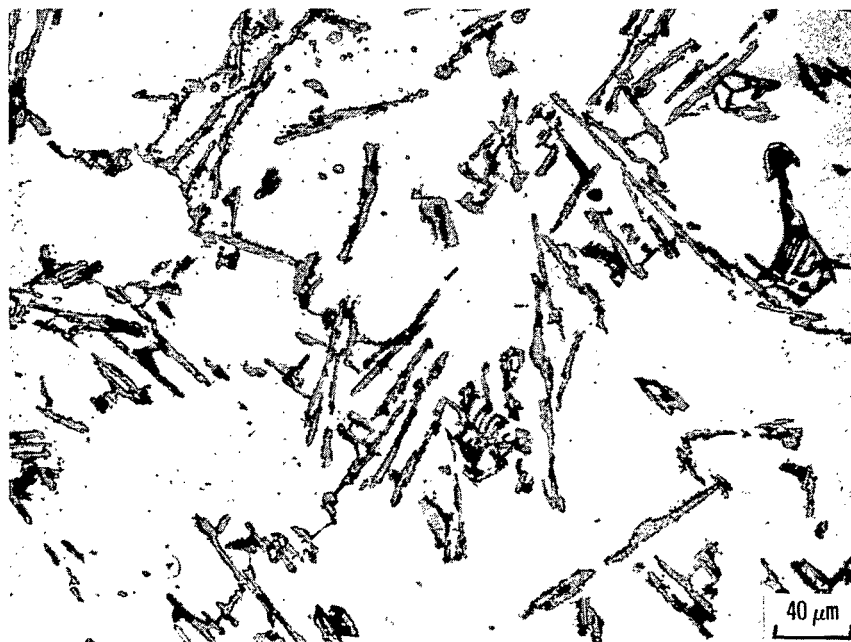
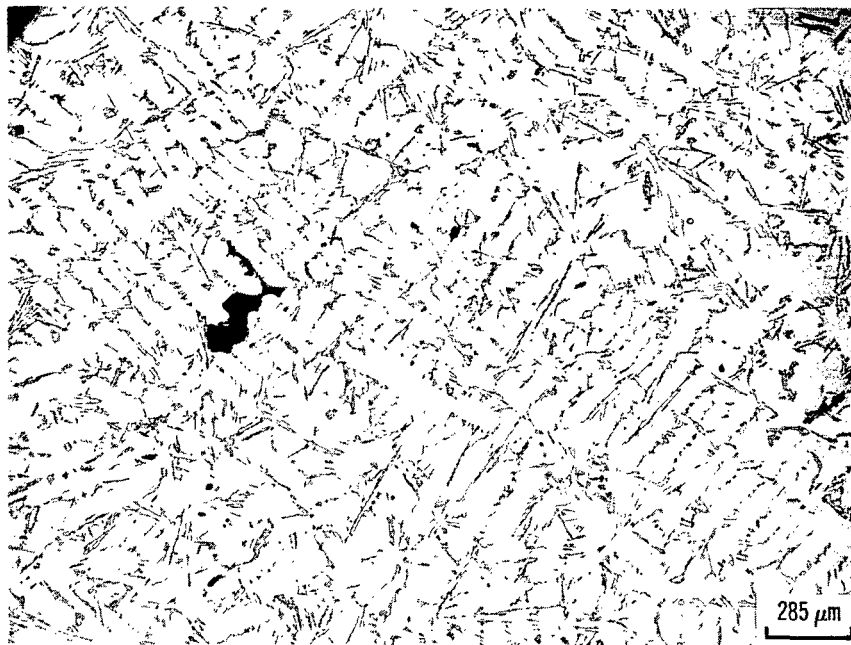
(a) Al-3Si.

Figure 2. - Photomicrographs of aluminum-silicon alloys.



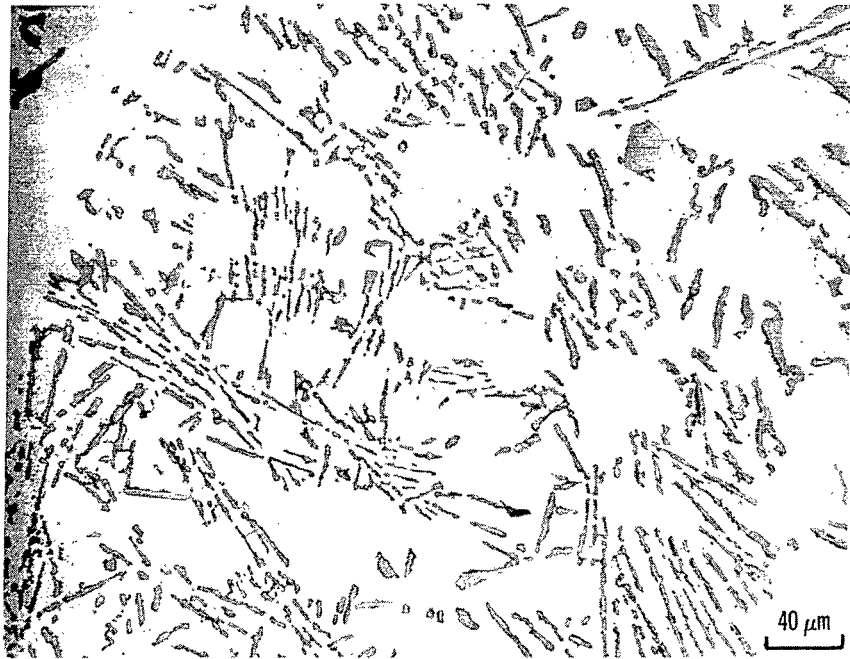
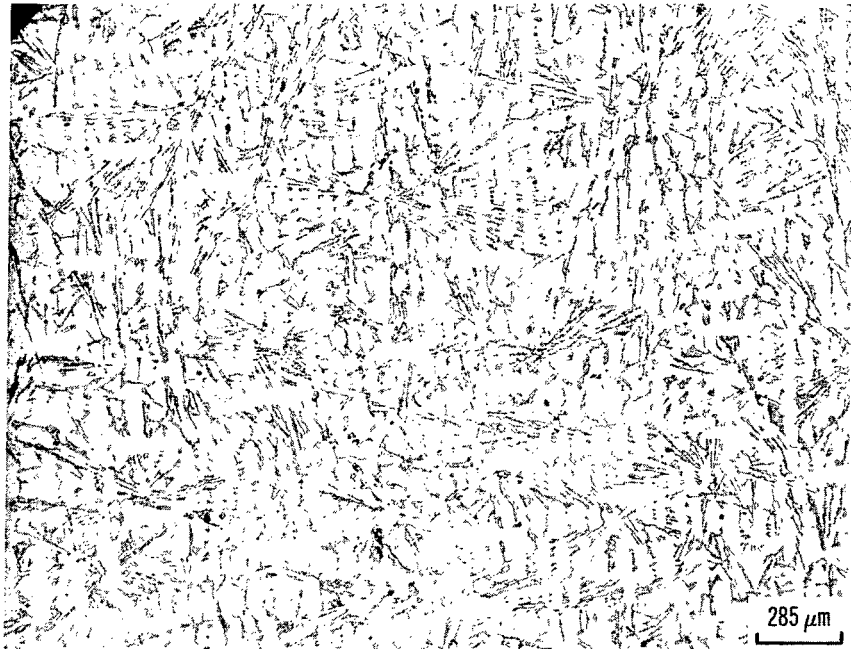
(b) Al-6Si.

Figure 2. - Continued.



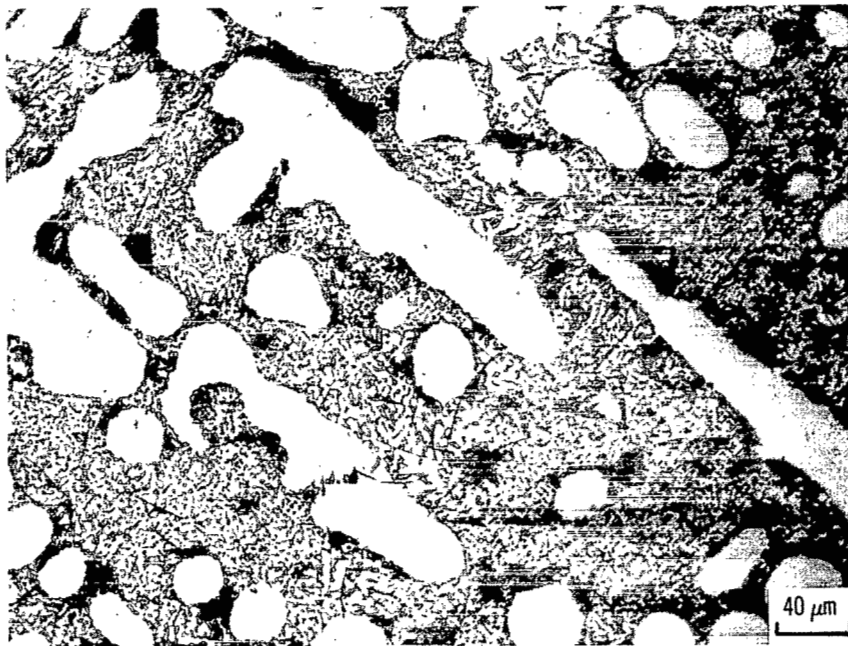
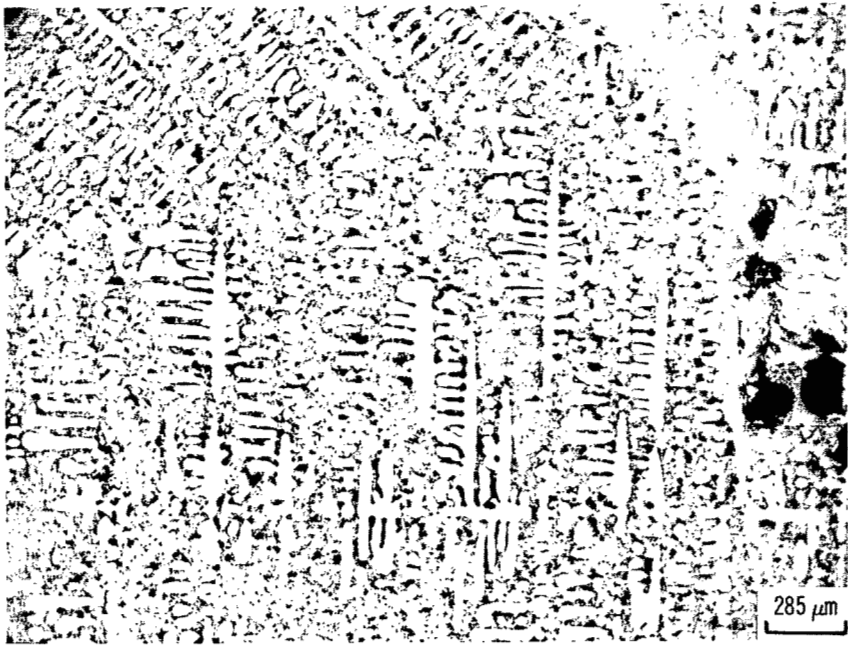
(c) Al-8Si.

Figure 2. - Continued.



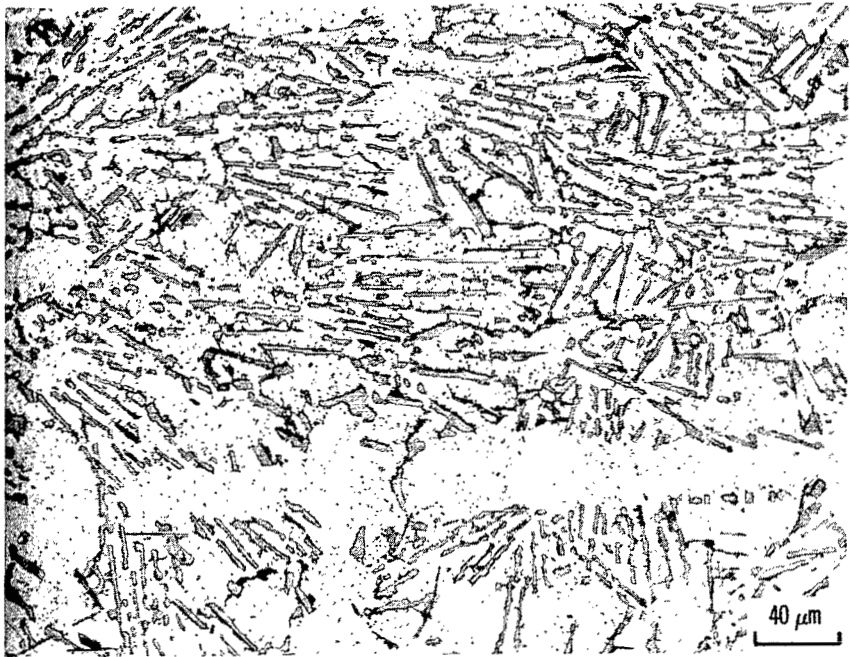
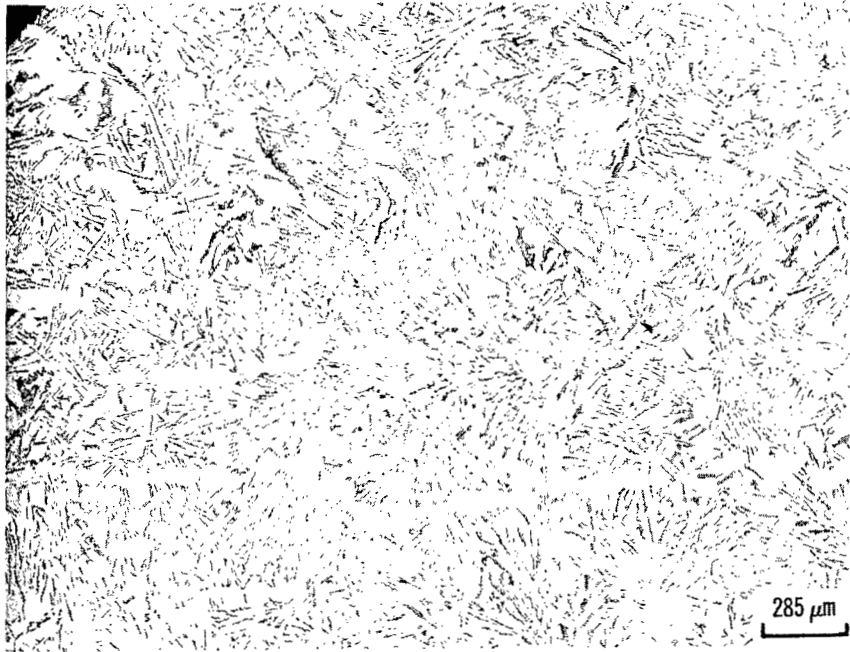
(d) Al-10Si.

Figure 2. - Continued.



(e) Al-10Si (Sr modified).

Figure 2. - Continued.



(f) Al-12Si.

Figure 2. - Concluded.

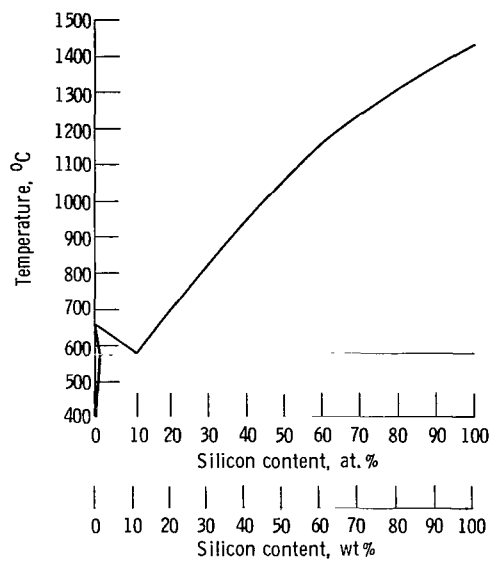
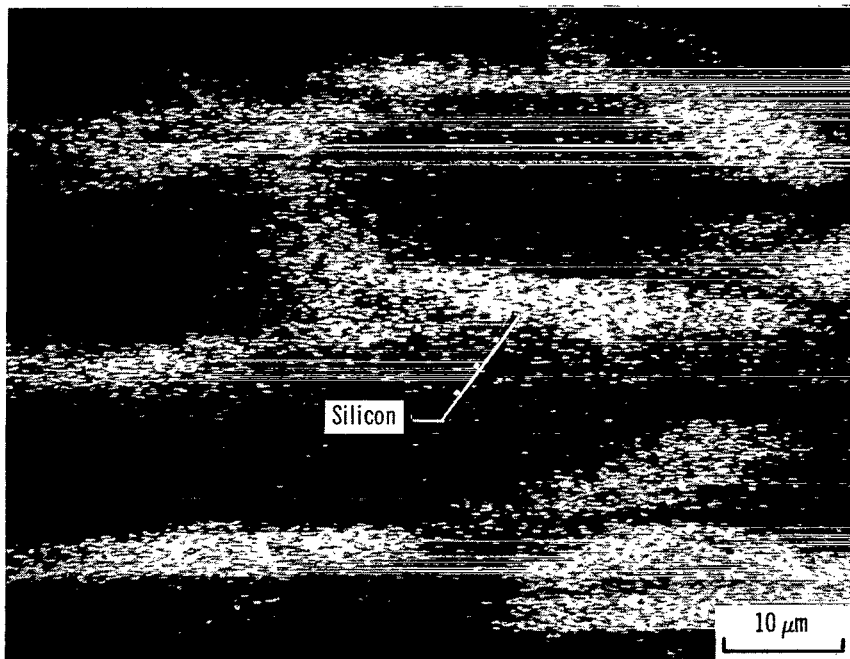


Figure 3. - Phase diagram for aluminum-silicon system. (From ref. 8.)



(a) SEM photograph.



(b) XDA image.

Figure 4. - Scanning electron microscope photograph and X-ray dispersive analysis image of Al-8Si alloy.

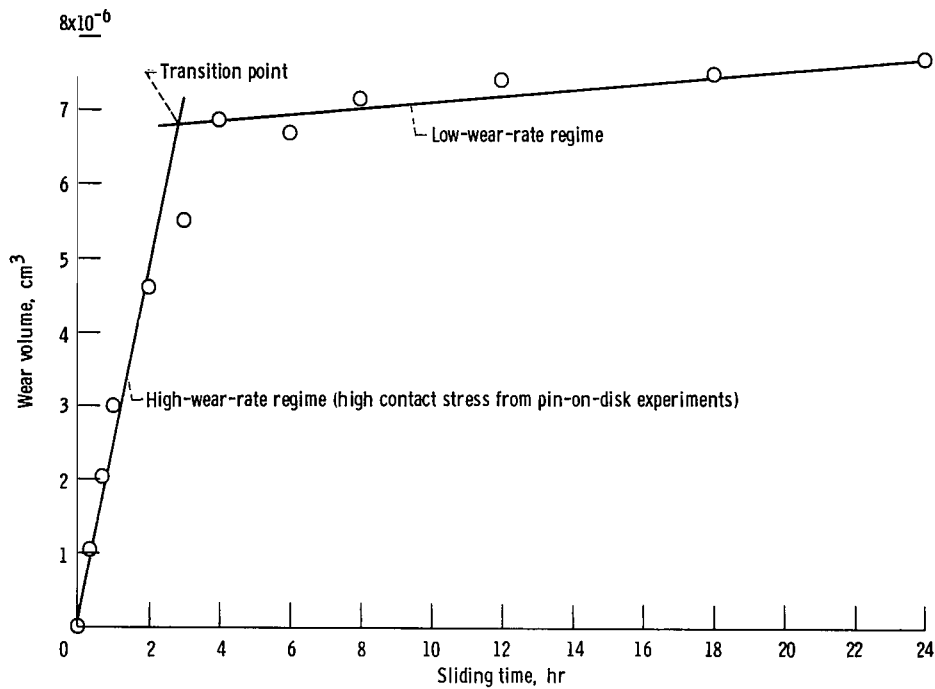


Figure 5. - Wear volume of Al-12Si as function of time. Sliding speed, 2.6 cm/sec; load, 500 g; lubricant, mineral oil.

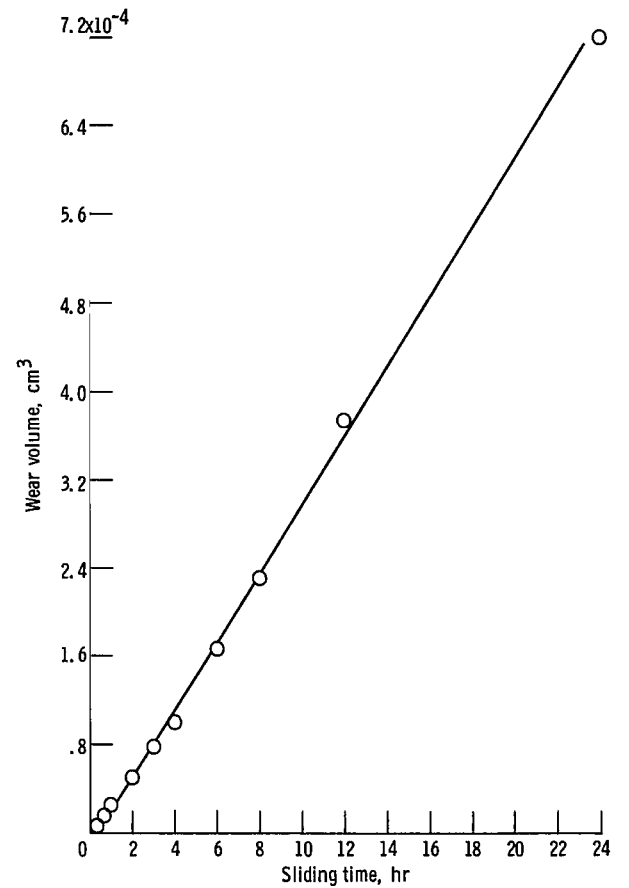
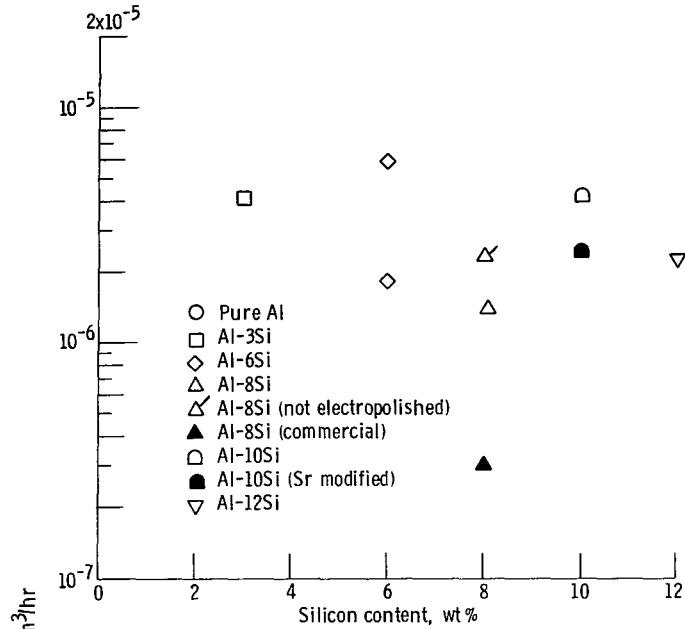
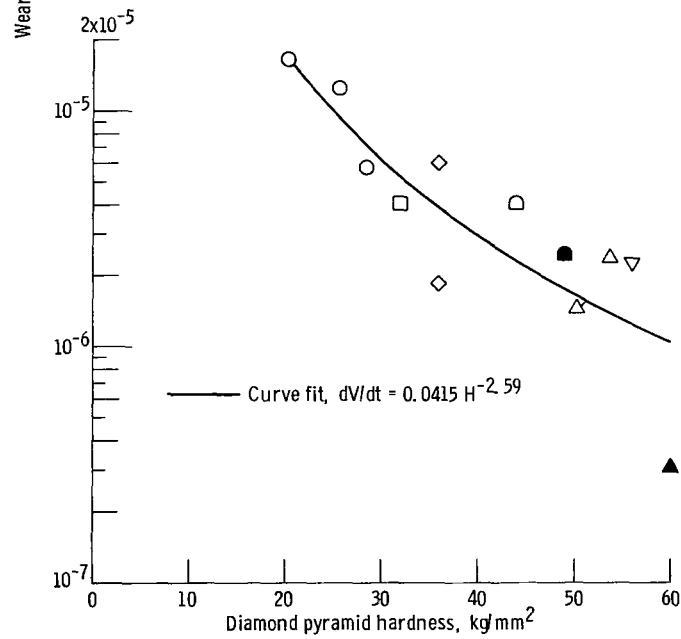


Figure 6. - Wear volume of pure aluminum as function of time. Sliding speed, 2.6 cm/sec; load, 500 g; lubricant, mineral oil.

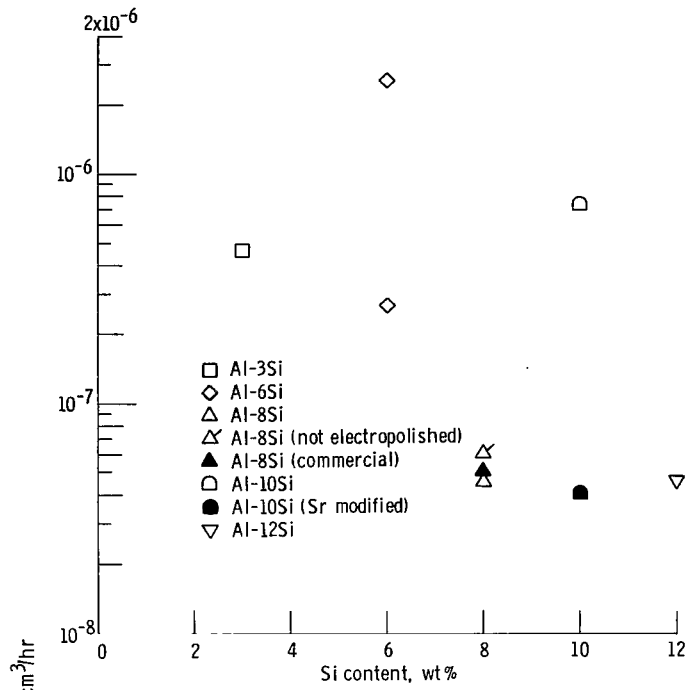


(a) Wear rate as function of silicon content.

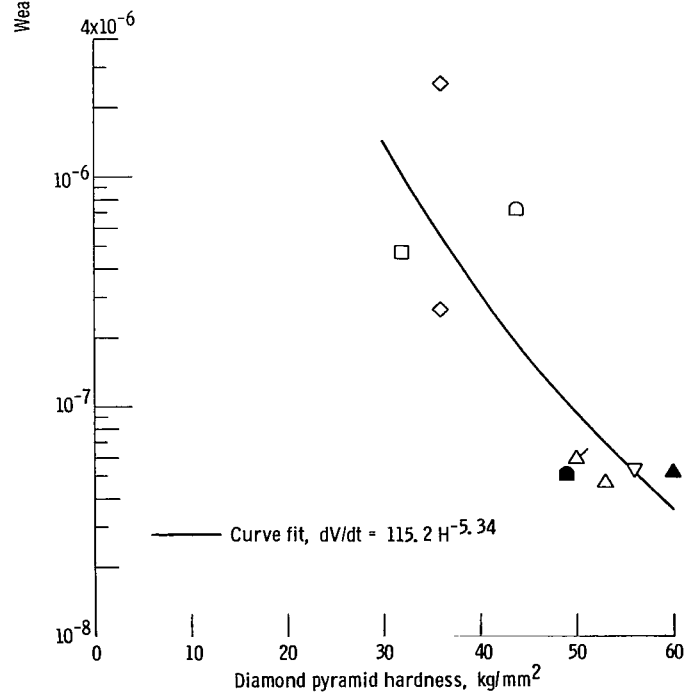


(b) Wear rate as function of hardness.

Figure 7. - Wear rate of aluminum and aluminum-silicon alloys as function of silicon content and hardness - high-wear-rate regime.

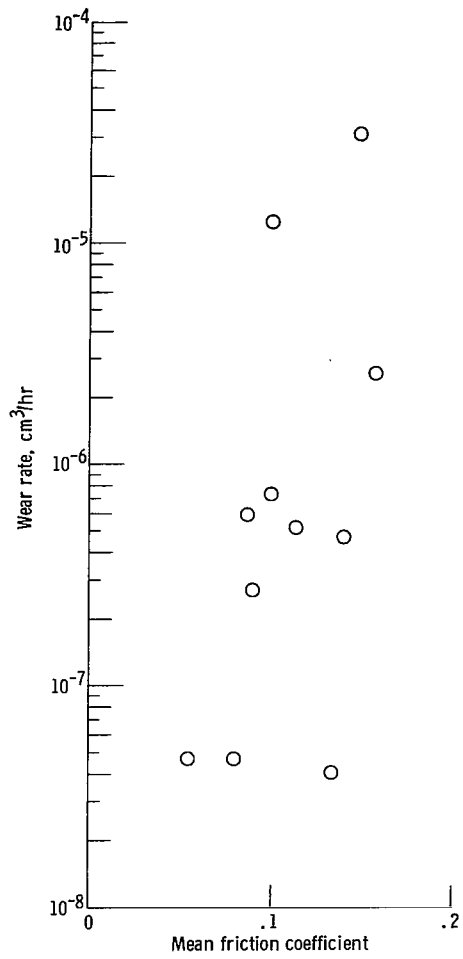


(a) Wear rate as function of silicon content.

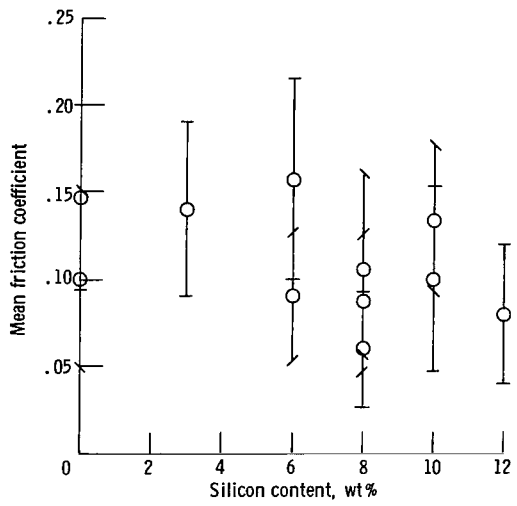


(b) Wear rate as function of hardness.

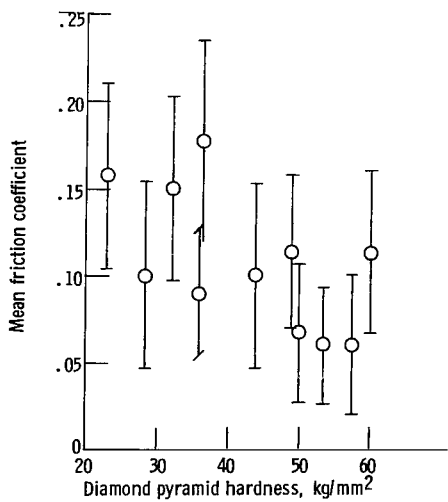
Figure 8. - Wear rate of aluminum and aluminum-silicon alloys as function of silicon content and hardness - low-wear-rate regime.



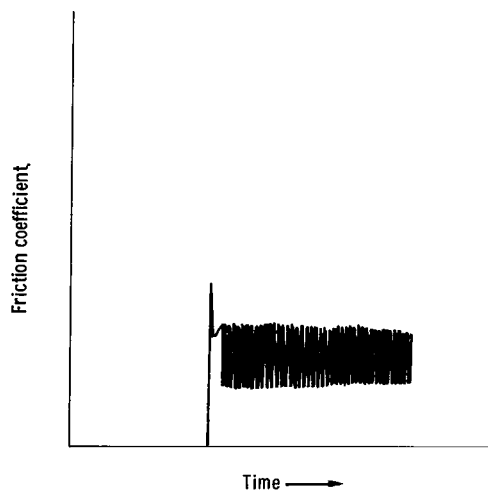
(a) Friction coefficient as function of wear rate.



(c) Friction coefficient as function of silicon content.



(b) Friction coefficient as function of hardness.



(d) Friction coefficient as function of time.

Figure 9. - Friction coefficient of aluminum-silicon alloys as function of wear rate, silicon content, hardness, and time.

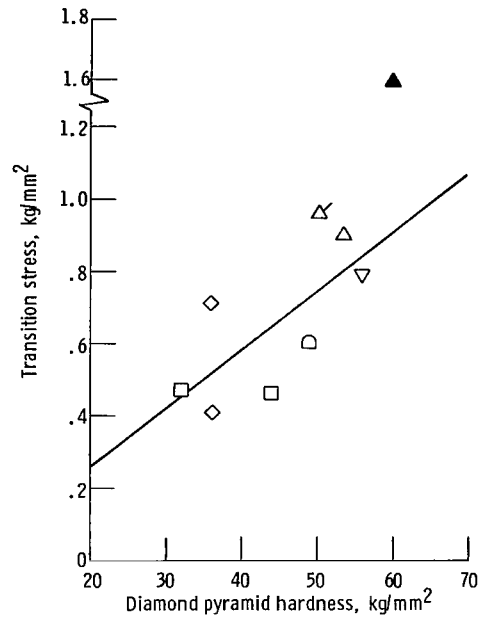
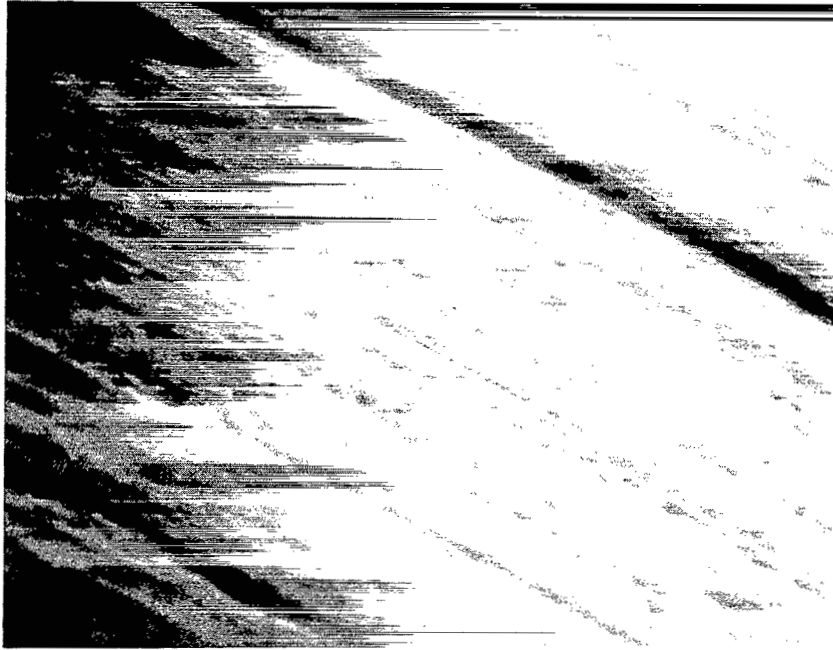
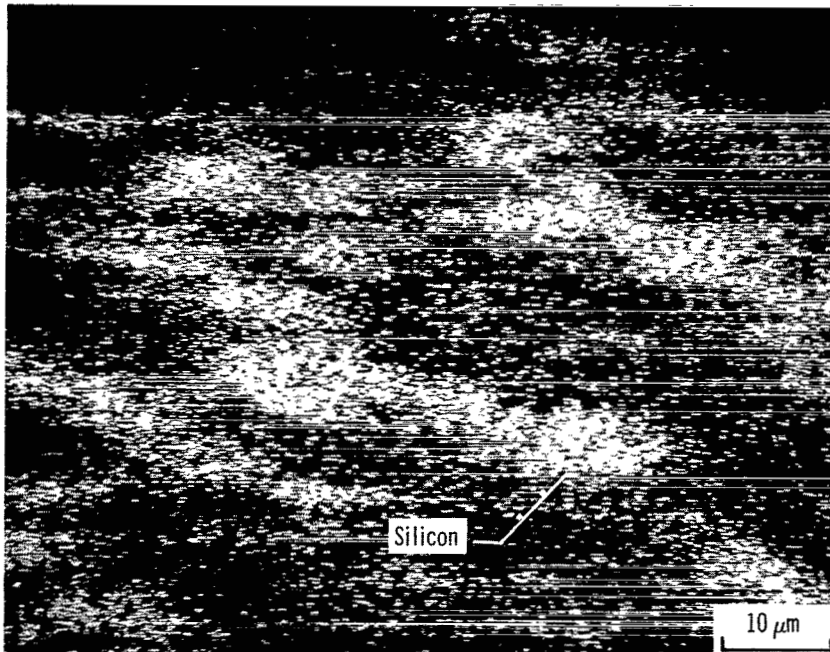


Figure 10. - Stress at transition from high- to low-wear-rate regime.

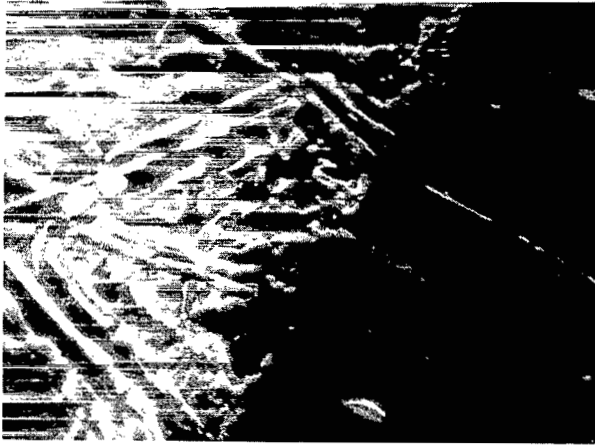


(a) SEM photograph.



(b) XDA image.

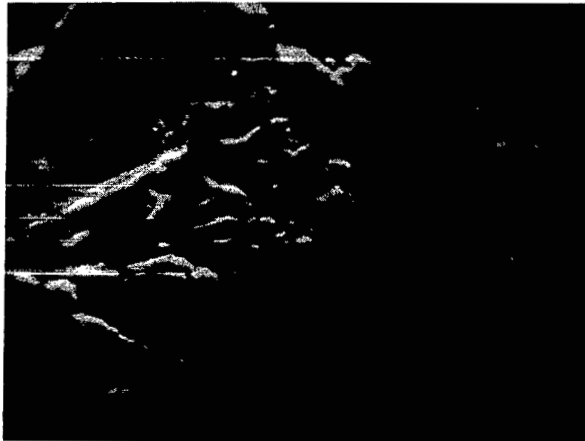
Figure 11. - Scanning electron microscope photograph and X-ray dispersive analysis image of worn Al-8Si alloy.



(a) SEM photograph after 200 revolutions.

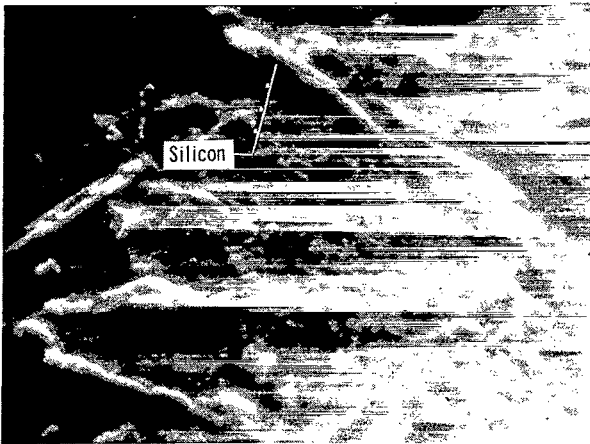


(b) SEM photograph after 2000 revolutions.

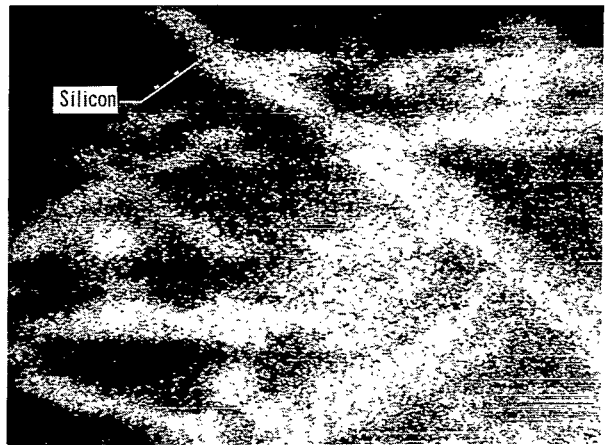


(c) SEM photograph after 3000 revolutions.

Figure 12. - Scanning electron microscope photographs and X-ray dispersive analysis image of wear scar on Al-8Si alloys as function of sliding distance.



(d) SEM photograph of alloy after 3000 revolutions (fig. 12(c)) and electropolishing.



(e) XDA image of alloy after 3000 revolutions and electropolishing (fig. 12(d)).

Figure 12. - Concluded.

1. Report No. NASA TP-1442		2. Government Accession No.		3. Recipient's Catalog No.	
4. Title and Subtitle <b>WEAR OF ALUMINUM AND HYPOEUTECTIC ALUMINUM-SILICON ALLOYS IN BOUNDARY-LUBRICATED PIN-ON-DISK SLIDING</b>				5. Report Date April 1979	
7. Author(s) <b>John Ferrante and William A. Brainard</b>				6. Performing Organization Code	
9. Performing Organization Name and Address <b>Lewis Research Center National Aeronautics and Space Administration Cleveland, Ohio 44135</b>				8. Performing Organization Report No. <b>E-9809</b>	
12. Sponsoring Agency Name and Address <b>National Aeronautics and Space Administration Washington, D.C. 20546</b>				10. Work Unit No. <b>506-16</b>	
15. Supplementary Notes				11. Contract or Grant No.	
16. Abstract				13. Type of Report and Period Covered <b>Technical Paper</b>	
<p>The friction and wear of pure aluminum and a number of hypoeutectic aluminum-silicon alloys (with 3- to 12-wt % Si) were studied with a pin-on-disk apparatus. The contacts were lubricated with mineral oil and sliding was in the boundary-lubrication regime at 2.6 cm/sec. Surfaces were analyzed with photomicrographs, scanning electron microscopy, X-ray dispersive analysis, and diamond pyramid hardness measurements. There were two wear regimes for the alloys - high and low - whereas pure aluminum exhibited a high wear rate throughout the test period. Wear rate decreased and the transition stress from high to low wear increased with increasing hardness. There was no correlation between friction coefficient and hardness. A least-squares curve fit indicated a wear-rate dependence greater than the inverse first power of hardness. The lower wear rates of the alloys may be due to the composites of silicon platelets in aluminum resulting in increased hardness and thus impairing the shear of the aluminum.</p>				14. Sponsoring Agency Code	
17. Key Words (Suggested by Author(s)) <b>Aluminum Silicon Alloys Wear studies</b>			18. Distribution Statement <b>Unclassified - unlimited STAR Category 26</b>		
19. Security Classif. (of this report) <b>Unclassified</b>		20. Security Classif. (of this page) <b>Unclassified</b>		21. No. of Pages <b>26</b>	22. Price* <b>A03</b>

National Aeronautics and  
Space Administration

THIRD-CLASS BULK RATE

Postage and Fees Paid  
National Aeronautics and  
Space Administration  
NASA-451



Washington, D.C.  
20546

Official Business

Penalty for Private Use, \$300

3 1 10,C, 033079 S00903DS  
DEPT OF THE AIR FORCE  
AF WEAPONS LABORATORY  
ATTN: TECHNICAL LIBRARY (SUL)  
KIRTLAND AFB NM 87117

**NASA**

POSTMASTER: If Undeliverable (Section 158  
Postal Manual) Do Not Return

---